Uluslararası İleri Doğa Bilimleri ve Mühendislik Araştırmaları Dergisi
Sayı 7, S. 89-99, 6, 2023

Araştırma Makalesi

International Journal of Advanced Natural Sciences and Engineering Researches
Volume 7, pp. 89-99, 6, 2023

Research Article

https://as-proceeding.com/index.php/ijanser
ISSN: 2980-0811

Effect of Plasma Nitriding Parameters on Microstructure and Mechanical Properties of DIN 1.2367 Hot Work Tool Steel

Ali ARI[1]

[1]*Department of Weapon Industry Technician, Vocational School of Higher Education, OSTİM Technical University, Ankara, TURKEY*

ali.ari@ostimteknik.edu.tr, https://orcid.org/0000-0003-2702-2982.

(Received: 03 July 2023, Accepted: 24 July 2023)

(5th International Conference on Applied Engineering and Natural Sciences ICAENS 2023, July 10 - 12, 2023)

ATIF/REFERENCE: Arı, A. (2023). Effect of Plasma Nitriding Parameters on Microstructure and Mechanical Properties of DIN 1.2367 Hot Work Tool Steel. *International Journal of Advanced Natural Sciences and Engineering Researches*, 7(6), 89-99.

Abstract – This study investigated the hardness and wear on DIN 1.2367 hot work tool steel after applying plasma nitriding processes under different conditions. The effect of the plasma nitriding process temperature and the N2:H2 gas mixture ratio was examined in the group of specimens investigated. In the plasma nitriding process applied to the group, the increase in the N2 ratio in the gas mixture significantly increased the hardness and wear properties of the material. In addition, the wear resistance of the specimen with the highest hardness value was increased.

Keywords - Plasma Nitriding, Friction Coefficient, DIN 1.2367 Tool Steel

I. INTRODUCTION

Tool steels are a type of high-alloy steels utilized for shaping and forming various materials. While tool steels can have varying carbon content, they contain higher proportions of alloying elements like chromium, molybdenum, tungsten, titanium, vanadium, nickel, and cobalt, depending on their specific applications. Through processes such as hardening and tempering, these steels acquire exceptional strength, toughness, and resistance to wear. Due to these advantageous characteristics, tool steels are extensively employed in the fabrication of dies, punches, injection molds, and sheet metal cutting and punching molds for both hot and cold forming operations. These applications involve contact conditions that lead to diverse wear mechanisms, often influenced by different tribological factors [1]. Hence, it is crucial for tool steels to possess elevated hardness, wear resistance, and superior mechanical properties. Additionally, tool steels intended for hot work applications must exhibit resistance to softening and retain their hardness at high temperatures. The microstructure of tool steel is highly dependent on the heat treatment process and is closely related to the material's wear resistance. Wei et al. focused on the friction, wear behavior, and wear mechanisms of heat-treated and tempered hot work tool steel under various sliding conditions and concluded that wear resistance was related to annealing conditions [2].

Leskovsek et al., on the other hand, studied the effect of austenitization and annealing temperatures on the hardness and fracture toughness of H11 hot work tool steel. The austenitization temperatures (1000, 1020, and 1050 °C) were observed when the specimens were tempered above the secondary hardening temperature. In these cases, significantly lower fracture toughness was obtained for specimens austenitized at 1000 °C and 1050 °C. In addition, after increasing the austenitization temperature, hardness was increased by quenching [3].

Surface modification is a prevalent industrial technique employed to enhance the longevity and performance of metals. Nitriding, a thermochemical surface treatment, plays a crucial role in improving fatigue strength, tribological characteristics, and corrosion resistance of materials. This process involves the diffusion of nitrogen species from various sources, resulting in the formation of nitrogen-enriched phases within the near-surface region [4]. The composition and thickness of these nitrided layers primarily rely on operating factors such as temperature and duration of the treatment, atmospheric conditions, and the composition of the substrate. Numerous research studies have highlighted the intimate connection between these parameters and the fatigue performance, tribological properties, and corrosion resistance of the treated materials [5].

Fernandes et al. subjected H13 steel to plasma nitriding at temperatures of 450, 550, and 650 °C. A diffusion zone was observed at the nitriding temperature of 450 °C, whereas a composite layer was produced at 550 °C and 650 °C. Both the surface and bulk hardness decreased as the nitriding temperature increased. In terms of wear and corrosion, it was concluded that a nitriding temperature of 450 °C or 550 °C led to better corrosion properties and that better wear performance was achieved at the nitriding temperature of 650 °C [6].

Soleimani et al. applied the plasma nitriding process to DIN 1.2210 steel under different temperature and time conditions. It was concluded that plasma nitriding had significantly improved the fatigue life of the steel. Fatigue strength increased with increasing plasma nitriding temperature and time [7]. Leite et al. subjected H13 tool steel discs to plasma nitriding at 400 °C in a mixture of 80% H2–20% N_2 gas for treatment times of 4 - 36 h. Results showed that longer nitriding time reduced wear volume [8]. Wen et al. applied plasma nitriding to plastic mold steel at 470, 500, and 530 °C for 4, 8, and 12 h under an atmosphere of 25% N2 + 75% H2. The amount of ε-nitride and total nitride increased with the increase in nitriding temperature and time. They found that the corrosion resistance of the material increased in parallel with the nitriding temperature and time [9]. Bhadraiah et al. applied the plasma nitriding process to Cr-MoV steel at 450 °C and 515 °C temperatures. They reported that the maximum surface hardness of about 1200 HV was reached at 515 °C and that the diffusion depth was ∼108 μm [10].

DIN 1.2367 (X38CrMoV5-3) is a widely utilized tool steel containing chromium and molybdenum. This steel type offers superior hot hardness and temper resistance compared to similar tool steels like AISI H11 and H13, primarily due to its higher molybdenum content. DIN 1.2367 has found significant application in various fields, including gear manufacturing, cutting tools, mandrel punches, and tool dies. It is favored for its remarkable combination of high hardness, toughness at elevated temperatures, and excellent resistance to wear and thermal fatigue. Numerous studies have extensively investigated the mechanical properties, frictional behavior, and wear characteristics of DIN 1.2367 tool steel, particularly in relation to the tempering process and its resulting microstructure [11]. In certain applications, this tool steel is subjected to intense cyclic plastic deformation, which can lead to microchipping and fracture. Consequently, a thorough understanding of its fatigue behavior is essential for comprehensive characterization.

Liu et al. conducted a series of systematic experiments to comprehensively investigate the impact of annealing and plasma nitriding treatments on the low-cycle fatigue behavior of DIN 1.2367 tool steel at both macroscopic and microscopic levels. They also proposed suitable approaches for estimating the fatigue life of this tool steel under different process conditions. The study revealed that the tempered condition exhibited the highest fatigue life at 580 °C, followed by 540 °C, while the lowest fatigue life was observed at 620 °C. However, the fatigue life differences among the three temper conditions were significantly reduced when plasma nitriding was applied, and the strain life curves nearly reached convergence. Fractography examinations of the fatigue-fractured surfaces of the plasma nitrided specimens showed brittle cracking with no apparent cracks. These findings provide valuable insights into the influence of annealing and plasma nitriding treatments on the low-cycle fatigue behavior of DIN 1.2367 tool steel [12].

DIN 1.2367 is widely employed in the metal forging industry as a hot work tool steel. To enhance its surface wear resistance, nitriding treatments are commonly utilized. Hence, this research focused on investigating the wear characteristics of DIN 1.2367 steel by subjecting it to plasma nitriding processes under various conditions, aiming to examine the steel's wear properties in relation to different nitriding parameters.

II. MATERIAL AND METHODS

The material utilized in this study was commercially accessible DIN 1.2367 (X38CrMoV5-3) hot work tool steel, having the chemical composition (% by weight) as outlined in Table 1. DIN 1.2367 finds common usage in various applications, including die-casting dies for light alloys (such as aluminum, zamak, brass, and magnesium) of small and medium sizes, molds and dies for thermosets and thermoplastic injection molding, as well as extrusion tooling for light alloys (such as liners, mandrels, pressure pads, extrusion stems, and dies). Additionally, it is employed in the forging and hot stamping of both light and heavy metals, closed dies, punches, stamps, jaws, hot rolling rolls, and hot cutting applications (including circular, straight, and angular cutting blades) [13].

Table 1. Nominal composition of the DIN 1.2367 hot work steel used in this study

C (%)	Si (%)	Mn (%)	P (%)	S (%)	Cr (%)	Mo (%)	V (%)
0.393	0.455	0.380	<0.03	<0.02	4.81	3.2	0.501

The selection of austenitizing temperatures was based on both the recommendations provided by the steel manufacturer and the need to ensure carbide stability. The recommended austenitizing temperature for DIN 1.2367 hot work tool steel is 1030 °C. To achieve this, the test specimens underwent a final preheating step in a horizontal vacuum furnace, reaching a temperature of 850 °C. Subsequently, they were heated to the desired austenitization temperature of 1030 °C, with a heating rate of 12 °C/min. The specimens were held at this temperature for 2 hours due to their specific wall thickness of 30 mm. For quenching, a nitrogen gas pressure of 45 bar was utilized, with a quenching rate of 3 °C/s. Lastly, tempering was conducted at 520 °C for 2 hours. These heat treatments resulted in the DIN 1.2367 hot work tool steel attaining a hardness of 50 HRC [14].

Three different nitriding processes were applied to the DIN 1.2367 hot work tool steel. Conditions of nitration are shown in Table 2. The Group specimens were placed on the cathode before the plasma nitriding (PN) process and vacuumed until the process chamber pressure was 2×10^{-2} mbar. Hydrogen gas was then introduced into the interior until the gas pressure was 2.5 mbar for the "scattering process", which would provide surface cleanliness and roughness suitable for nitriding. Scattering was carried out at 250 ºC treatment temperature for 30 min. Following this process, 80% H_2, 20% N_2 for the first specimen, 80% H_2, 20% N_2 for the second specimen, and a fixed gas mixture of 20% H_2, 80% N_2 for the third specimen were given into the vacuum chamber, and nitriding was carried out at a process pressure of 2.5 mbar. Plasma nitriding processes were applied at two different temperatures for 10 h. The application temperature was 540 °C for the first specimen, 500 °C for the second, and 500 ºC for the third. After the nitriding process was completed, nitrogen gas at 3 mbar was injected into the vacuum chamber. The specimens were cooled to room temperature in a vacuum environment.

Table 2. Plasma nitriding test parameters

Test Specimens	Temperature	Time	N_2:H_2	Pressure
PN1	540 °C	10 h	1:4	250 Pa
PN2	500 °C	10 h	1:4	250 Pa
PN3	500 °C	10 h	4:1	250 Pa

To examine the microstructure and hardness distribution, the initial material as well as the treated and nitrided specimens underwent a polishing procedure using various grit sizes of sandpaper (180, 320, 400, 600, and 1000) in a polishing device. Following the sanding process, a broadcloth and diamond pastes with particle sizes of 6 µm and 1 µm were utilized for further polishing. This sequence of sanding and polishing steps allowed for the preparation of the specimens, ensuring a suitable surface finish for microstructural analysis and hardness measurements. The microstructure analysis was conducted using a Nikon LV 150 light microscope. To measure the hardness, the Metkon MH-3 Vickers hardness-testing machine was employed, which had a load range of 0.01-1 kg. The hardness tests were performed with a 50-g load applied for a duration of 10 seconds. Hardness measurements were taken at specific depths of 50, 100, 150, 200, 250, and 300 µm from the surface of the specimens. Five measurements were taken for each depth, and the average value was calculated. In this study, the nitriding depth was determined based on the DIN 50 190/3 standard, which defined it as the depth at which the hardness value exceeded the core hardness by 50 HV. The wear tests were performed under dry friction conditions without removing any wear product residues. Two different friction speeds were selected: 12.4 mm/s and 5 mm/s. The applied load was set at 15 N, and data acquisition was conducted for a duration of 4 seconds. The trace diameter was determined to be 18 mm. Prior to each wear test and afterward, the specimens were weighed using a precise scale to measure the mass loss during the test. The total wearing distance covered during the tests was 45 m.

III. RESULTS AND DISCUSSION

A. Microstructure and hardness

Figure 1 illustrates the microstructure of DIN 1.2367 tool steel in its original state (AR) and after undergoing heat treatment (HT). In Figure 1a, the AR microstructure is composed of ferrite and pearlite phases. Figure 1b reveals the presence of small precipitate particles in the tempered steel, accompanied by an internal structure consisting of martensite phase. Although the DIN 1.2367 steel exhibited enhancements, the occurrence of martensite phase in the internal structure was attributed to the limited duration of the curing process.

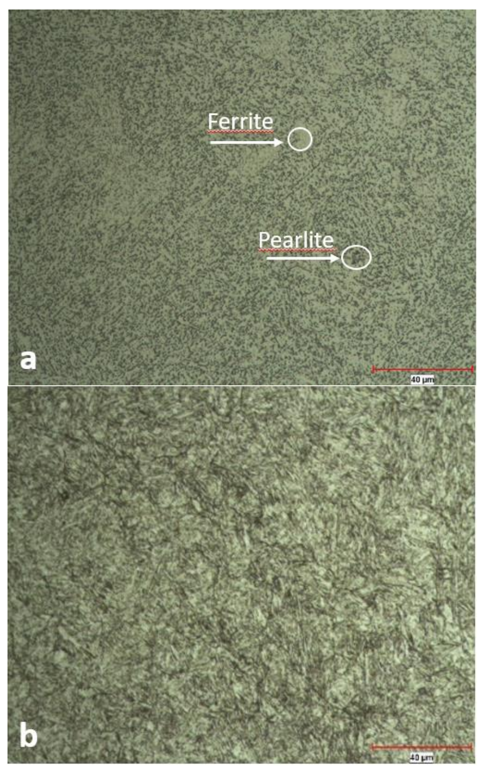

Fig. 1 Microstructure of DIN 1.2367 tool steel under the optical microscope: a) AR, b) HT

The microstructure images depicted in Figures 2-6 showcase two distinct regions beneath the surface: the diffusion layer and the matrix region. The matrix region exhibits a martensitic structure. Upon closer examination of the matrix region, the presence of precipitate particles can be observed within the internal structure. The following aspects will be taken into account: 1) the influence of plasma nitriding temperature on DIN 1.2367 hot tool steel while maintaining constant gas-mixing ratios and 2) the impact of the gas mixture while keeping the plasma nitriding temperature constant. Figures 2 and 3 show the cross-section of the Group PN1 and PN2 specimens under an optical microscope. The thickness of the diffusion layer of the PN1 specimen subjected to plasma nitriding at 540 °C at a constant N2/H2 (1:4) ratio was 215.7 µm (Figure 2a), and the thickness of the diffusion layer of the PN2 specimen subjected to plasma nitriding at 500 °C was 188.8 µm (Figure 3a). As was expected, a deeper diffusion layer was observed at high nitriding temperatures. In the nitriding at 500 °C, there was a weak contrast between the surface region and the core of the specimen. Microhardness measurements were applied to confirm the transition between the diffusion zone and the inner core. At 550 °C, a more intense contrast can be observed between the surface region and the core of the specimen. The nitrided layer contains fine iron nitrides inside the grains and at the grain boundaries. It is impossible to distinguish the compact composite layer from the main diffusion layer, and needle-like iron nitrides arise in the nitrided layer at both processing temperatures. However, the white layer is slightly more pronounced in the nitrided specimens at 550 °C (Figures 2b and 3b). At a constant temperature of 500 °C, the thickness of the diffusion layer was 188.8 µm with the N2/H2 ratio of 1:4 (Figure 3a), whereas the thickness of the diffusion layer was 215.7 µm with the N2/H2 ratio of 4:1 (Figure 4a). In the plasma nitriding process performed by Podgornik et al. on an AISI H11 workpiece, it was observed that the thickness of the diffusion layer increased when the N2 ratios were raised [4], thus supporting the results obtained in our study. Nitriding at 500 °C with the N2/H2 ratio of 4:1 (Figure 4b) resulted in a thin white surface layer plus a thick diffusion zone. In this case, distinction between the diffusion zone and the substrate was more apparent. Additionally, thin elongated precipitates caused by grain boundary precipitation were seen in the diffusion zone. As shown in Figures 3-4, when plasma nitriding takes place at the N2/H2 ratio of 1:4 and 500 °C, no white layer is formed, but at the N2/H2 ratio of 4:1 and 500 °C, a white layer is formed. This indicates that the thickness of the white layer depends on the nitrogen-hydrogen ratio. The studies of Saulo and Lu support this situation [15,16].

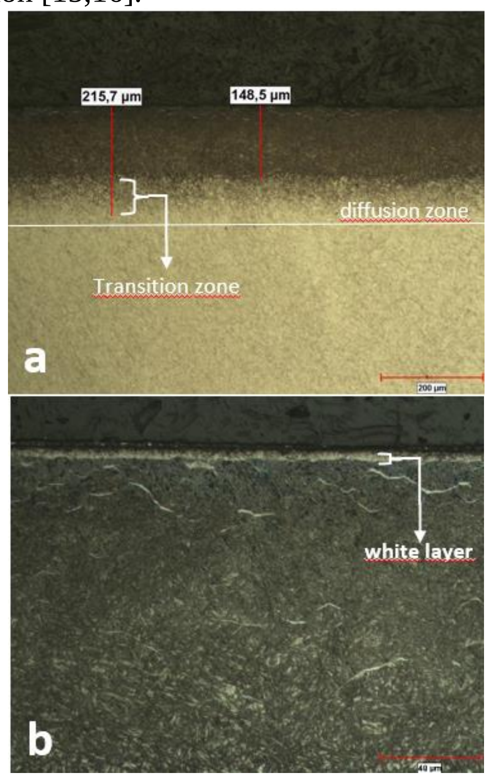

Fig. 2 Optical microscope images of the plasma-nitrided specimen PN1 at 540 ºC for 10 h (N2/H2:1/4)

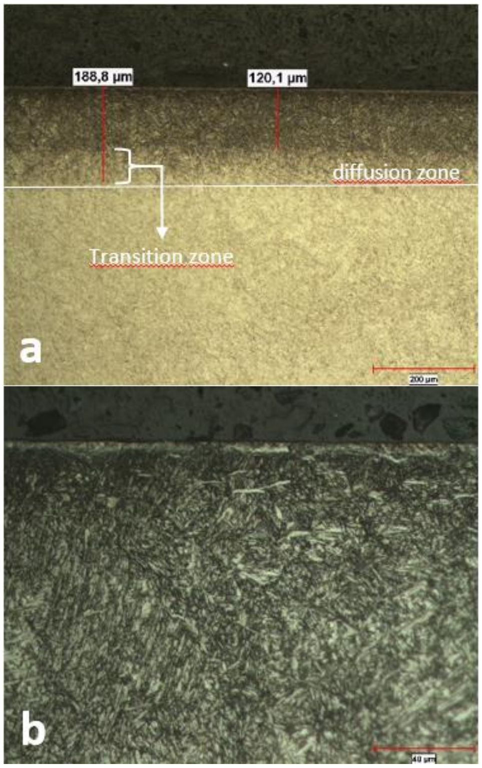

Fig. 3 Optical microscope images of the plasma-nitrided specimen PN2 at 500 ºC for 10 h (N2/H2:1/4)

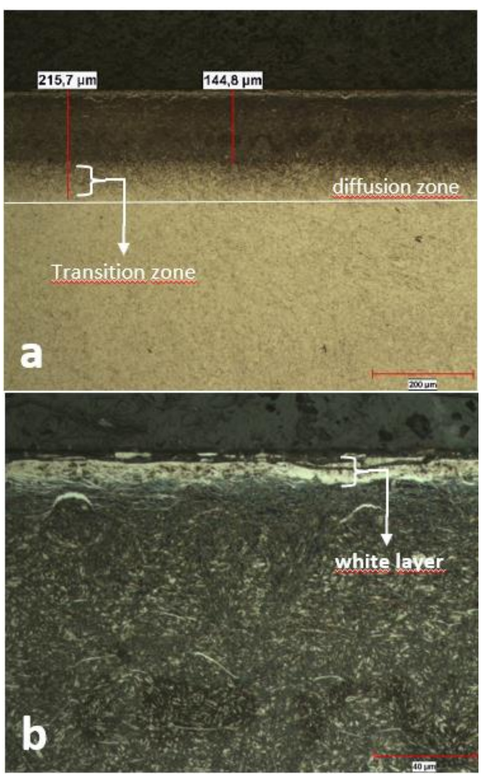

Fig. 4 Optical microscope images of the plasma-nitrided specimen PN3 at 500 ºC for 10 h (N2/H2:4/1)

B. *Hardness measurements*

The mean hardness of the initial material was determined to be 196.28 HV, while that of the tempered steel was found to be 514.46 HV. Figure 5 illustrates a decrease in the surface hardness of the materials as the nitriding temperature rises. The hardness value of PN2 was 1088.16 HV and that of PN1 was 1040.72 HV. Karimzadeh et al. investigated the effect of time and temperature on the plasma nitriding behavior of AISI H13 hot work tool steel. They applied the nitriding process with a 25% N_2-75% H_2 gas mixture and showed that the near-surface hardness decreased with the increase of the treatment temperature [17]. Forati Rad et al. encountered similar results and attributed this to the exposure of the steel substrate to the effect of increased tempering [18]. In the present study, the surface hardness of the PN2 specimen, which was nitrided at 540 °C, was reduced because it was subjected to increased tempering. The enhanced hardness of the formed nitrided layer was ascribed to the formation of well-dispersed CrN precipitates, which contributed to the elevated surface hardness. The higher chromium content led to an increased density of CrN precipitation on the surface, further contributing to the maximum surface hardness [19].

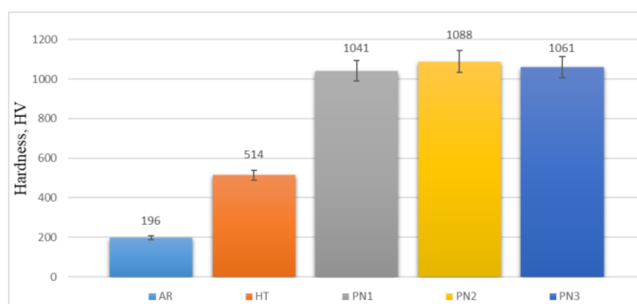

Fig. 5 Hardness results of the test specimens

The hardness distribution and nitriding depth of the plasma nitrided PN1 and PN2 specimens are shown in Figure 6. The hardness distribution of the PN1 and PN2 specimens indicates that the increase in nitriding temperature did not cause a significant change in the hardness distribution. Bhadraiah et al. applied the plasma nitriding process to specimen number one at 515 °C for 10 h. and specimen number two at 450 °C for 10 h and observed that the hardness distribution of the specimens was very similar [10]. Podgornik et al. found that altering the plasma activation markedly affected the hardness distribution [4]. With the plasma nitriding process, nitrogen ions diffuse inward from the material surface forming a nitrided zone. Nitrogen dissolves in steel as interstitial atoms and forms precipitates of alloying elements and nitrides. Nitride precipitates (chrome, molybdenum, vanadium nitride, etc.) disrupt the lattice, create stress fields due to incompatibility with the matrix structure, and compress the dislocations, resulting in a significant increase in hardness. Therefore, when the N_2 ratio is increased in the plasma nitriding process, the thickness and hardness of the diffusion layer of the material also increase [19]. In our study, when the PN2 and PN3 specimens were compared, the N_2/H_2 ratio of the PN2 specimen was 1:4, and that of the PN3 specimen was 4:1. The intense nitriding atmosphere (N_2 = 80%) significantly increased the hardness distribution [20].

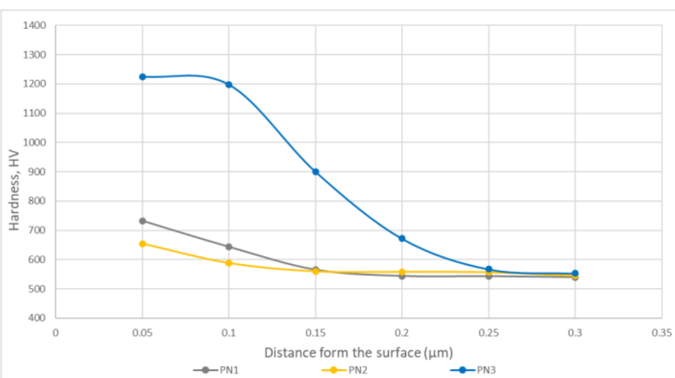

Fig. 6 Hardness distribution of plasma- and gas-nitrided DIN 1.2367 steel specimens

C. Wear resistance

The graphs illustrating the changes in friction coefficient during the wear tests are presented in Figures 9 to 18 for a load of 15 N. Both the starting material and nitrided specimens exhibited a rapid initial increase in the friction coefficient, followed by a transition to a stable, steady-state condition after a short duration (Figures 9 - 18). The plasma nitriding results show that the friction properties were improved, with the lowest friction values found in the PN3 specimen (Figure 13). During friction, hard, abrasive particles are released, disrupting the contact conditions. Thus, the coefficient of friction changes and the abrasive wear character emerges (Figures 13 - 16). This situation was also reported in the study of Karaoğlu [21]. The results of tests performed at a 15-N load and 5-mm/s and 12.4-mm/s sliding speeds show similar characteristics. When the friction coefficients were compared, they were found to be directly related to the surface hardness. The friction coefficients of specimen PN3, which have roughly equal hardness distribution at 0.05 µm, were the lowest. Because the hardness distribution of PN1 and PN2 at 0.05 µm was roughly equal, the friction coefficients were also very similar in these two specimens. The initial friction coefficient value of these specimens was high due to surface roughness, but was then reduced to a steady value after about 10 m of sliding distance [8]. Because of the high hardness of the sublayer, the oxide layers were protected and acted as a solid lubricant that was very effective in reducing the contact area, which decreased the friction coefficient and the wear rate of these specimens [22,23]. Considering that the nitriding process temperatures of PN1 and PN2 were 500 °C and 550 °C, respectively, the 50 °C nitriding process temperature difference had no significant effect on the friction coefficient. However, increasing the N2 ratio in the gas mixture to 4:1 significantly improved the friction coefficient.

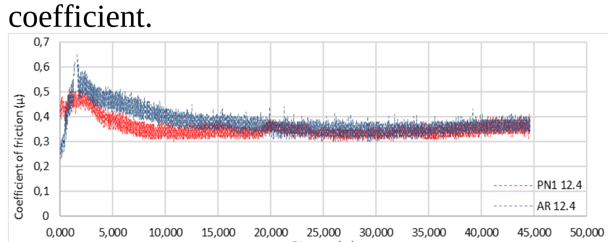

Fig. 7 Friction coefficient changes of AR and PN1 specimens at 12.4 mm/s sliding speed

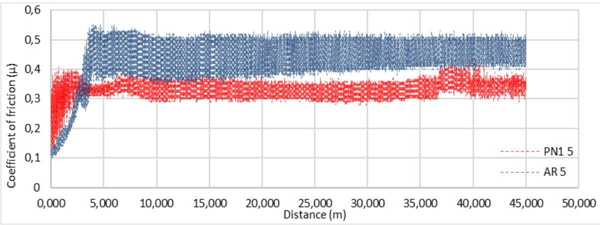

Fig. 8 Friction coefficient changes of AR and PN1 specimens at 5 mm/s sliding speed

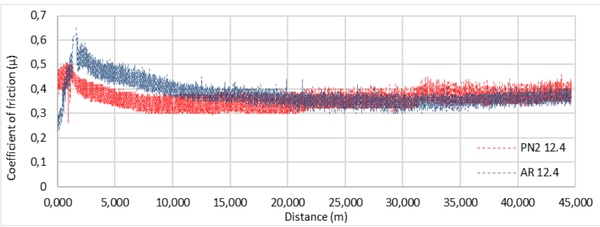

Fig. 9 Friction coefficient changes of AR and PN2 specimens at 12.4 mm/s sliding speed

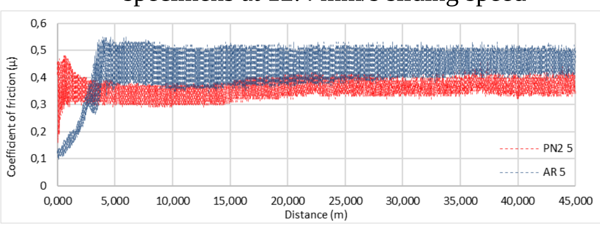

Fig. 10 Friction coefficient changes of AR and PN2 specimens at 5 mm/s sliding speed

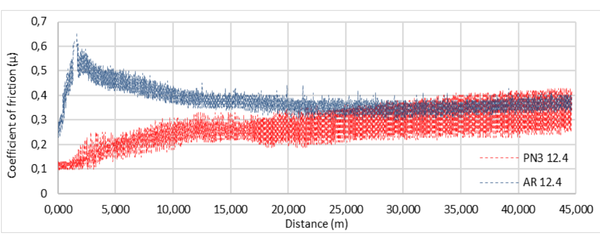

Fig. 11 Friction coefficient changes of AR and PN3 specimens at 12.4 mm/s sliding speed

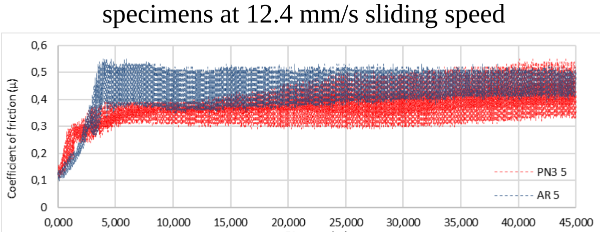

Fig. 12 Friction coefficient changes of AR and PN3 specimens at 5 mm/s sliding speed

Based on the determined nitriding type and parameters in this study, Figures 13 to 16 clearly demonstrate that the wear resistance of the DIN 1.2367 steel after nitriding was significantly superior to that of the as-received (AR) material. The wear test specimen PN3 at a friction speed of 12.4 mm/s (Figure 16a) displayed the smallest wear trace, measuring 2.7 times smaller than the wear trace of the as-received (AR) specimen (Figure 13). Upon examining the microscopic images of the AR specimen, it is evident that both adhesive and abrasive wear are present. When the wear areas of the analyzed specimens are compared, the nitration process is shown to contribute to the tribological properties of the specimens. With the applied load, the hard and brittle structure formed caused fractures and abrasive fragments. Intense abrasive and adhesive wear can be seen in the microstructure images. In addition, since the wear products were not removed during the experiment, the particles in question acted to increase the wear in the test system. Figures 13 - 16 show that these particles adhered to the test specimen with abrasive effects causing the formation of cavities. The PN3 specimen exhibited the lowest amount of wear trace, i.e., the best wear resistance was seen in the PN3 specimen. This was because of the intense nitriding atmosphere (N_2 = 80%). The highest hardness was seen in the PN3 specimen at a depth of 0.15 µm, which provided high wear resistance just below the surface. Therefore, it exhibited higher resistance to abrasion compared to the other specimens.

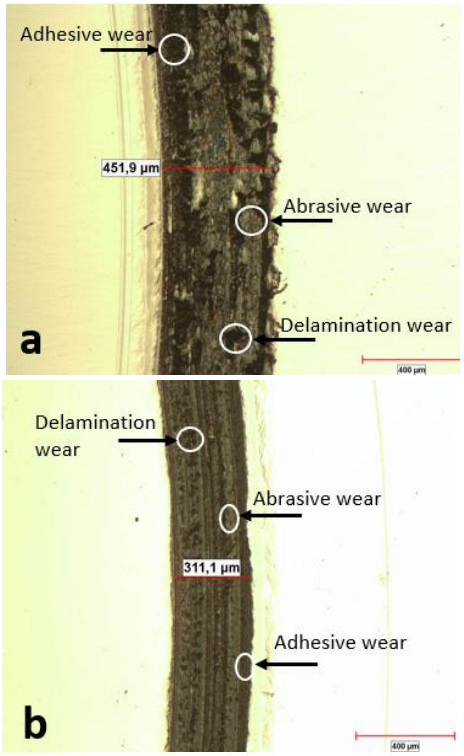

Fig. 13 Optical microscope images of the wear groove and track width for AR specimen: (a) 12.4 mm/s, (b) 5 mm/s

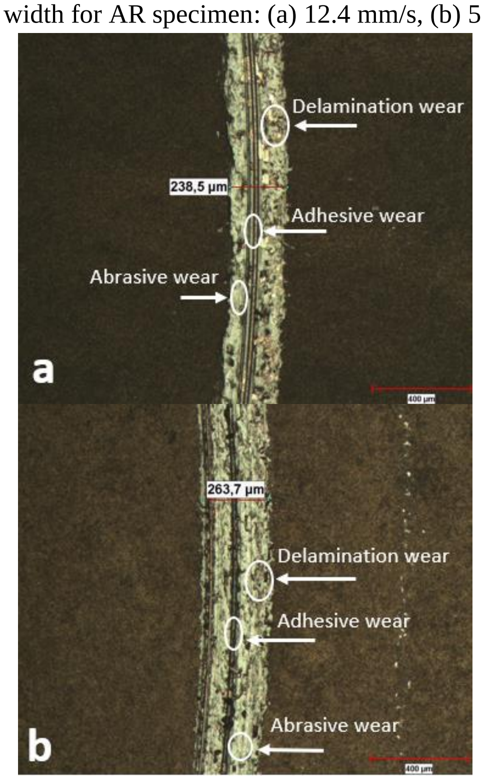

Fig. 14 Optical microscope images of the wear groove and track width for PN1 specimen: (a) 12.4 mm/s, (b) 5 mm/s

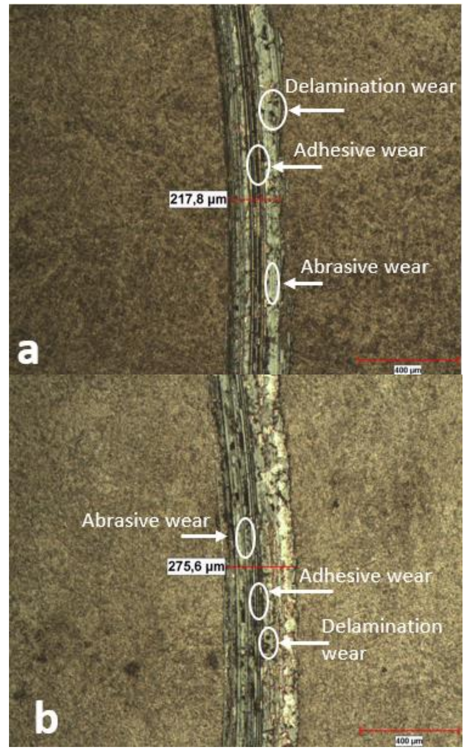

Fig. 15 Optical microscope images of the wear groove and track width for PN2 specimen: (a) 12.4 mm/s, (b) 5 mm/s

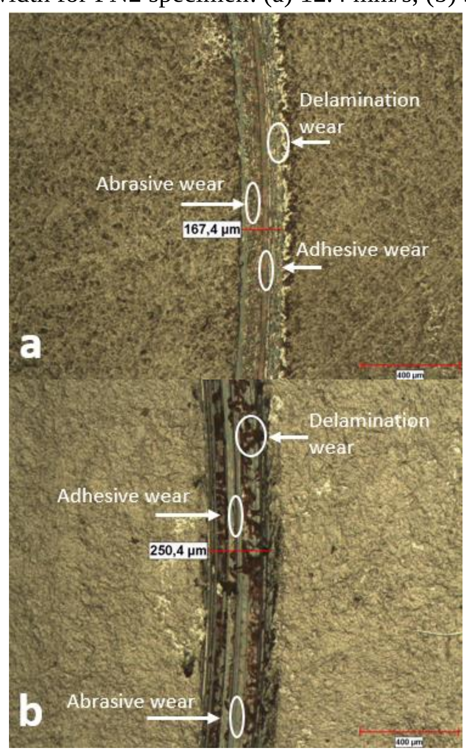

Fig. 16 Optical microscope images of the wear groove and track width for PN3 specimen: (a) 12.4 mm/s, (b) 5 mm/s

IV. CONCLUSION

The objective of this study was to investigate how the hardness, depth of diffusion, and wear characteristics of DIN 1.2367 hot work tool steel are influenced by varying nitriding conditions.

The surface hardness decreased with increased temperature of the plasma nitriding process. This reduction in hardness was attributed to the high-temperature tempering of the substrate. The hardness distribution in the layers of the PN3 specimen (with plasma nitriding conditions of 500 °C and the N_2:H_2 gas mixture ratio of 4:1) was higher than for PN1 and PN2.

When the N_2 ratio in the N_2/H_2 gas mixture was increased from 1:4 to 4:1 in the plasma nitriding process, the diffusion layer and hardness values increased significantly.

A white layer was formed in the PN3 specimen at 500 °C with the N_2/H_2 gas mixture ratio of 4:1. However, no white layer was formed in the PN2 specimen at 500 °C with the N_2/H_2 gas mixture ratio of 1:4.

The nitriding hardening of the DIN 1.2367 hot work tool steel significantly contributed to the wear resistance property of the material compared to the untreated steel.

The wear properties were very close at the nitriding temperatures of 500 °C and 540 °C. However, as seen in the PN3 specimen, when the N_2 in the N_2/H_2 gas mixture ratio was increased from 1:4 to 4:1, the friction coefficient and wear traces were significantly reduced, with the lowest friction coefficient and wear trace observed in the PN3 specimen.

REFERENCES

[1] G. Carasi, B. Yu, E. Hutten, H. Zurob, R. Casati, M. Vedani, Effect of Heat Treatment on Microstructure Evolution of X38CrMoV5-1 Hot-Work Tool Steel Produced by L-PBF, Metall. Mater. Trans. A Phys. Metall. Mater. Sci. 52 (2021) 2564–2575. https://doi.org/10.1007/s11661-021-06248-y.

[2] M.X. Wei, S.Q. Wang, L. Wang, X.H. Cui, K.M. Chen, Effect of tempering conditions on wear resistance in various wear mechanisms of H13 steel, Tribol. Int. 44 (2011) 898–905. https://doi.org/10.1016/j.triboint.2011.03.005.

[3] V. Leskovšek, B. Šuštaršič, G. Jutriša, The influence of austenitizing and tempering temperature on the hardness and fracture toughness of hot-worked H11 tool steel, J. Mater. Process. Technol. 178 (2006) 328–334. https://doi.org/10.1016/j.jmatprotec.2006.04.016.

[4] B. Podgornik, V. Leskovšek, F. Tehovnik, J. Burja, Vacuum heat treatment optimization for improved load carrying capacity and wear properties of surface engineered hot work tool steel, Surf. Coatings Technol. 261 (2015) 253–261. https://doi.org/10.1016/j.surfcoat.2014.11.021.

[5] B. Skela, M. Sedlaček, F. Kafexhiu, B. Podgornik, Wear behaviour and correlations to the microstructural characteristics of heat treated hot work tool steel, Wear. 426–427 (2019) 1118–1128. https://doi.org/10.1016/j.wear.2018.12.032.

[6] F.A.P. Fernandes, S.C. Heck, C.A. Picone, L.C. Casteletti, On the wear and corrosion of plasma nitrided AISI H13, Surf. Coatings Technol. 381 (2020) 125216. https://doi.org/10.1016/j.surfcoat.2019.125216.

[7] S.M.Y. Soleimani, A.R. Mashreghi, S.S. Ghasemi, M. Moshrefifar, The effect of plasma nitriding on the fatigue behavior of DIN 1.2210 cold work tool steel, Mater. Des. 35 (2012) 87–92. https://doi.org/10.1016/j.matdes.2011.09.067.

[8] M. V. Leite, C.A. Figueroa, S.C. Gallo, A.C. Rovani, R.L.O. Basso, P.R. Mei, I.J.R. Baumvol, A. Sinatora, Wear mechanisms and microstructure of pulsed plasma nitrided AISI H13 tool steel, Wear. 269 (2010) 466–472. https://doi.org/10.1016/j.wear.2010.04.037.

[9] D.C. Wen, Microstructure and corrosion resistance of the layers formed on the surface of precipitation hardenable plastic mold steel by plasma-nitriding, Appl. Surf. Sci. 256 (2009) 797–804. https://doi.org/10.1016/j.apsusc.2009.08.062.

[10] D. Bhadraiah, C. Nouveau, B. Veeraswami, K. Ram Mohan Rao, Plasma based nitriding of tool steel for the enhancement of hardness, Mater. Today Proc. 46 (2021) 940–943. https://doi.org/10.1016/j.matpr.2021.01.185.

[11] I.Y. Malik, U. Lorenz, A. Chugreev, B.A. Behrens, Microstructure and wear behaviour of high alloyed hot-work tool steels 1.2343 and 1.2367 under thermo-mechanical loading, IOP Conf. Ser. Mater. Sci. Eng. 629 (2019). https://doi.org/10.1088/1757-899X/629/1/012011.

[12] C.C. Liu, J.H. Wu, C.C. Kuo, Low-cycle fatigue of

DIN 1.2367 steels in various treatments, Fract. Nano Eng. Mater. Struct. - Proc. 16th Eur. Conf. Fract. 387 (2006) 217–218. https://doi.org/10.1007/1-4020-4972-2_106.

[13] M. Bischof, P. Staron, D. Caliskanoglu, H. Leitner, C. Scheu, H. Clemens, On the overaging behaviour of tool steel X38 CrMoV 5-3, Mater. Sci. Eng. A. 472 (2008) 148–156. https://doi.org/10.1016/j.msea.2007.03.014.

[14] E.N.D.I.N. Esr, RV-2367 Hot Work Tool Steel RV-2367 ESR, (n.d.) 1–4.

[15] S.C. Lima, R. Hinrichs, M.A.Z. Vasconcellos, The influence of nitrogen to hydrogen ratio and temperature on thickness and phase composition in plasma nitrided Ti-6AL-4V, Rev. Mater. 24 (2019). https://doi.org/10.1590/S1517-707620190001.0607.

[16] L. Song, T. Peng, X. Zhao, J. Hu, Effect of nitrogen hydrogen ratio on plasma nitriding for 38CrMoAl, Acta Metall. Slovaca. 24 (2018) 229–233. https://doi.org/10.12776/ams.v24i3.1155.

[17] S. Karimzadeh, F. Mahboubi, G. Daviran, Plasma nitriding behavior of din 1.2344 hot work tool steel, Iran. J. Mater. Sci. Eng. 17 (2020) 1–9. https://doi.org/10.22068/IJMSE.17.4.1.

[18] H. Forati Rad, A. Amadeh, H. Moradi, Wear assessment of plasma nitrided AISI H11 steel, Mater. Des. 32 (2011) 2635–2643. https://doi.org/10.1016/j.matdes.2011.01.027.

[19] S. Mridha, A.A. Khan, The effects of process variables on the hardness of nitrided 3% chromium steel, J. Mater. Process. Technol. 201 (2008) 325–330. https://doi.org/10.1016/j.jmatprotec.2007.11.142.

[20] M. Tosun, L. Trabzon, Plazma nitrürleme işleminin 316l ostenitik paslanmaz çeliğinin malzeme özelliklerine mikro ve nano etkisi, (2012).

[21] S. Karaoğlu, Structural characterization and wear behavior of plasma-nitrided AISI 5140 low-alloy steel, Mater. Charact. 49 (2003) 349–357. https://doi.org/10.1016/S1044-5803(03)00031-7.

[22] J. Yang, Y. Liu, Z. Ye, D. Yang, S. He, Microstructural and tribological characterization of plasma- and gas-nitrided 2Cr13 steel in vacuum, Mater. Des. 32 (2011) 808–814. https://doi.org/10.1016/j.matdes.2010.07.022.

[23] R.L. Liu, M.F. Yan, Improvement of wear and corrosion resistances of 17-4PH stainless steel by plasma nitrocarburizing, Mater. Des. 31 (2010) 2355–2359. https://doi.org/10.1016/j.matdes.2009.11.069.